

# Three-Dimensional Analysis of Septal Curvature from Cardiac Magnetic Resonance Images for the Evaluation of Severity of Pulmonary Hypertension

F Maffessanti<sup>1,2</sup>, MA Sciancalepore<sup>1</sup>, AR Patel<sup>1</sup>, M Gomberg-Maitland<sup>1</sup>, S Chandra<sup>1</sup>, EG Caiani<sup>2</sup>, BH Freed<sup>1</sup>, RM Lang<sup>1</sup>, V Mor-Avi<sup>1</sup>

<sup>1</sup>University of Chicago, Chicago, Illinois, USA

<sup>2</sup>Politecnico di Milano, Milan, Italy

## Abstract

*Although abnormal motion of the interventricular septum (IVS) caused by elevated right ventricular pressure in patients with pulmonary hypertension (PH) is easy to recognize visually, determination of the severity of PH relies on measurements of pulmonary arterial pressure (PAP). We hypothesized that quantitative 3D analysis of regional IVS curvature throughout the cardiac cycle could be used to differentiate patients with different degrees of PH. Cardiac magnetic resonance (CMR) images (Philips 1.5T) were obtained in 14 normal subjects and 30 patients with PH undergoing right heart catheterization, who were divided into 3 subgroups according to mean PAP. Images were used to reconstruct dynamic 3D LV endocardial surfaces, which were analyzed to calculate 3D IVS curvature throughout the cardiac cycle. In normal subjects, IVS curvature was positive, reflecting the convex septal shape and showed little change throughout the cardiac cycle. In patients with PH, IVS curvature was lower, reflecting septal flattening, and fluctuated throughout the cardiac cycle, reflecting the abnormal “bouncing” septal motion. In patients with severe PH, IVS curvature reached negative values, reflecting transient concave septal shape. Dynamic 3D analysis of IVS curvature from CMR images may provide an alternative for noninvasive assessment of severity of PH.*

## 1. Introduction

Analysis of left ventricular (LV) shape using global indices, such as sphericity, has been useful in the evaluation of ventricular remodeling in a variety of disease states. However, when ventricular shape is affected regionally, such as flattening and abnormal dyssynergic motion of the interventricular septum (IVS) in pulmonary hypertension (PH), the value of global shape indices is limited. Although cardiac magnetic resonance (CMR) imaging is currently the standard reference

technique for the evaluation of both left and right ventricular (RV) volumes and function, current CMR tools do not include accurate, load-independent evaluation of the severity of PH, which requires direct measurement of pulmonary arterial pressure. This is currently achieved by either invasive catheter-based techniques or echocardiographic quantification of tricuspid regurgitation [1,2], which may at times be difficult and/or unreliable.

Several recent studies have reported significant relationships between septal curvature derived from CMR images and pulmonary arterial pressures [3,4] or vascular resistance [5]. These studies measured septal curvature in a single slice at one or two phases of the cardiac cycle. We hypothesized that 3D analysis of IVS curvature throughout the cardiac cycle could more accurately reflect the dynamic shape of the IVS and its relationship with pulmonary pressure and resistance. Accordingly, we developed a technique for 3D analysis of regional endocardial curvature and used it to test this hypothesis.

## 2. Methods

### 2.1. Population

We studied 44 adult patients, including 30 patients (age 53±14 yrs) with suspected PH, who underwent right heart catheterization and CMR imaging as well as 2D and Doppler echocardiography, and 14 patients with normal LV and RV function were used as normal controls (NL; age: 51±18 years). Patients with PH were divided into 3 subgroups according to the mean arterial pulmonary pressure (MPAP): mild (25-34 mmHg), moderate (35-50 mmHg) and severe (>50 mmHg). Exclusion criteria were standard contraindications to MRI. We did not exclude patients with severe tricuspid regurgitation, RV volume overload or RV hypertrophy.

### 2.2. Right heart catheterization

Right heart catheterization was performed as usual standard of care. After venous access was established, a

balloon-directed thermolodulation catheter was placed in the venous circulation and advanced into the pulmonary artery. Pressures were recorded and cardiac output was measured in order to calculate pulmonary vascular resistance (PVR) as:  $(\text{MPAP} - \text{pulmonary capillary wedge pressure})/\text{cardiac output}$ .

### 2.3. Echo evaluation of RV pressure

Echocardiographic imaging was performed using a commercial system (iE33, Philips, S3 transducer) from an apical window. Images were analyzed off-line (Philips EnConcert). RV systolic pressure (RVSP) was estimated using standard methodology [1]. Briefly, tricuspid regurgitant flow was identified by color flow Doppler, and the maximum jet velocity was measured by continuous wave Doppler. RVSP was estimated based on the modified Bernoulli equation and was considered to be equal to the systolic pulmonary arterial pressure in the absence of RV outflow obstruction:  $\text{RVSP (mmHg)} = \text{trans-tricuspid valve gradient} + \text{right atrial pressure}$ . Trans-tricuspid valve gradient was calculated as  $4v^2$ , where  $v$  = peak velocity of tricuspid regurgitation in m/sec, and the right atrial pressure was derived from the inferior vena cava dimensions and its collapsibility [1,6].

### 2.4. CMR imaging

CMR images were obtained using a 1.5 Tesla scanner (Philips) with a phased-array cardiac coil. Retrospectively gated steady-state free precession cine sequences with 30 images per cardiac cycle were acquired. After parallel short-axis slices was obtained from above the ventricular base to below the apex, three long-axis planes depicting the 2-, 3- and 4-chamber views were acquired.

### 2.5. Global size, function and shape

LV and RV endocardial borders were semi-automatically traced throughout the cardiac cycle using commercial software (MR Cardiac Analysis, ViewForum, Philips). Papillary muscles and endocardial trabeculae were included in the ventricular cavity. These borders were used to calculate LV and RV volumes throughout the cardiac cycle, from which end-diastolic and end-systolic volumes (EDV and ESV) and ejection fractions, LV EF and RV EF, respectively, were obtained.

### 2.6. 3D endocardial surface detection

The entire set of short- and long-axis images was analyzed using 4D-LV Analysis MR software (TomTec), as depicted in figure 1. End-diastole was identified as the first frame in the sequence, and end-systole as the frame depicting the smallest LV cavity. For each of these two frames, LV endocardial boundary was manually initialized in each of the three long-axis views (figure 1, left), while including the papillary muscles and endocardial trabeculae in the LV cavity. Then, the endocardial surface was reconstructed by finding the best fit to the endocardial boundaries throughout the cardiac cycle. Subsequently, the reconstructed surface was superimposed on the original long-axis images and its position was adjusted frame-by-frame by an experienced investigator. Finally, spatio-temporal smoothing was performed to avoid discontinuities. The resultant dynamic endocardial surface (figure 1, center) was exported as a series of connected meshes for custom analysis of LV endocardial curvature. In addition, end-systolic and end-diastolic values of LV sphericity index were recorded.

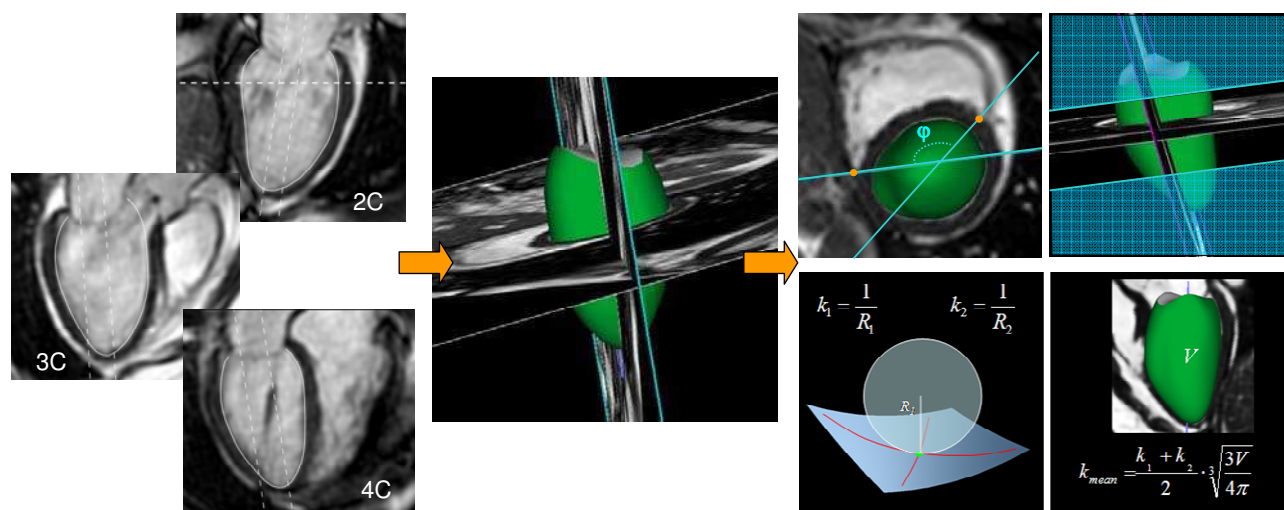


Figure 1. Schematic representation of the 3D reconstruction of LV endocardial surface. Following manual initialization of the endocardial contours at end-systole and end-diastole in three long-axis views (left: two-, three- and four-chamber views), 3D endocardial surface was reconstructed throughout the cardiac cycle and superimposed on the original images (center). Calculation of 3D septal curvature (right, see text for detail).

## 2.7. 3D curvature analysis

Custom software was used for analysis of regional LV endocardial curvature, (figure 1, right). First, for each node on the connected mesh representing the LV endocardial surface a quadric polynomial function was locally fitted to approximate a smooth surface [7]. Then, septal region of interest was defined at the mid ventricular level by a sector defined by the 2 insertion points of the RV free wall and by excluding approximately 20% of the LV length at both base and apex (shaded areas). For each point within this septal region, we calculated maximum curvature  $k_1$ , defined as the inverse of  $R_1$ , the radius of the smallest circle that would fit into the surface at that particular point, and the curvature  $k_2$  in the perpendicular direction. Mean 3D curvature was calculated for each point as the mean of  $k_1$  and  $k_2$ . Then, septal 3D curvature was obtained by averaging all points within the septal region. Finally, septal 3D curvature was normalized by mean LV curvature, defined as  $(\text{mean radius})^{-1}$  calculated from instantaneous LV volume, in order to compensate for changes in IVS curvature secondary to changes in LV size, resulting in size-normalized mean 3D septal curvature,  $k_N$ .

## 3. Results

3D analysis of septal curvature throughout the cardiac cycle was fully automated and required approximately 10 seconds on a standard personal computer, once the

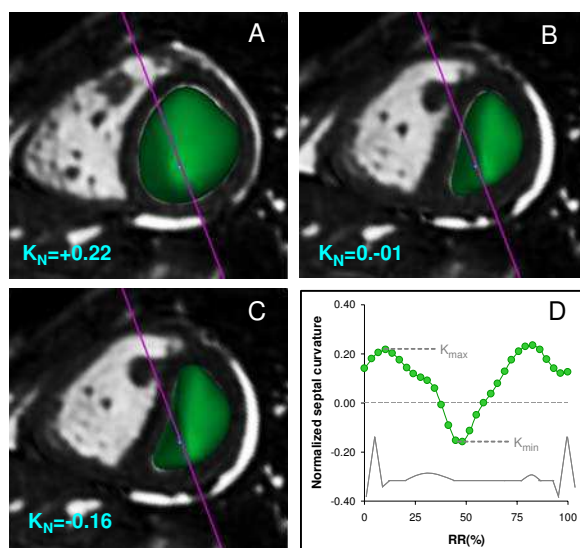


Figure 2. Example of 3D endocardial surface at difference phases of the cardiac cycle in a patient with PH: the septum is bowing towards the RV cavity, resulting in positive size-normalized curvature,  $k_N$  (A), then becomes flat, resulting in near zero  $k_N$  (B) and even bows towards the LV cavity, resulting in negative  $k_N$  (C). Curvature time curve (D) depicts these changes in septal shape throughout the cardiac cycle.

reconstruction of the dynamic LV endocardial surface using the commercial software was complete.

While there were no differences between groups in LV EF, RV EF gradually decreased with the severity of PH. Although end-diastolic sphericity index showed a trend of decrease with the severity of PH, the end-systolic sphericity index did not show a clear pattern, despite markedly decreased sphericity in the severe PH group.

In normal subjects, the time curves of 3D septal curvature were positive, reflecting the convex septal shape (bowing into the right ventricle) and showed little change throughout the cardiac cycle. In contrast, in patients with PH, IVS curvature was lower, reflecting septal flattening, and fluctuated throughout the cardiac cycle, reflecting the abnormal “bouncing” septal motion. In patients with severe PH, the normalized IVS curvature reached negative values, reflecting transient concave septal shape (bowing into the left ventricle). Figure 2 shows an example of 3D LV endocardial surface reconstructed from images obtained in a patient with severe PH at three different phases of the cardiac cycle, along with the corresponding time curve of  $k_N$ .

Averaged time curves of septal curvature depicted different temporal patterns of changes in septal shape in the four groups of patients (figure 3, A). Analysis of mean, minimum and maximum curvature values resulted in differences between the groups, reflecting progressively decreasing curvature with increasing severity of PH (figure 3, B-D), although the differences between the moderate and severe PH groups were not statistically significant.

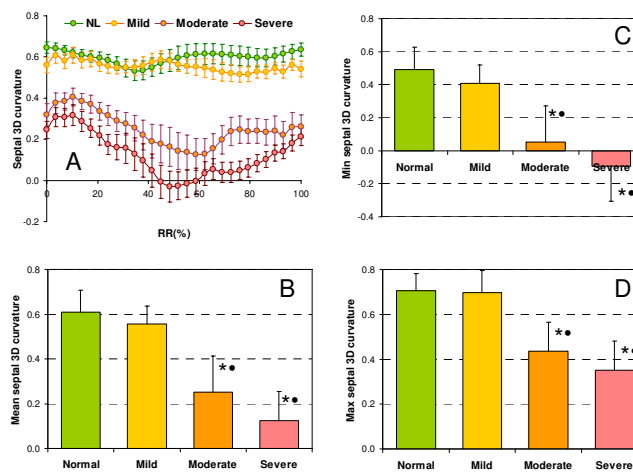


Figure 3. (A) Time curves of LV size normalized septal curvature calculated for patients in the four groups (average values shown with standard errors of the mean rather than SD to avoid overlap of error bars between groups). (B through D) Mean, minimum and maximum curvature values in the four groups. See text for details. \*  $p < 0.05$  vs Normal (NL), •  $p < 0.05$  vs Mild (analysis of variance).

Regression analysis between the mean septal 3D curvature,  $k_{\text{mean}}$ , and the invasive data obtained during the right heart catheterization in the 30 patients with PH showed strong linear relationships between the variables. Mean septal 3D curvature correlated well with pulmonary arterial pressures ( $r$ : 0.78 for MPAP and 0.79 for SPAP). The correlation with PVR was even higher ( $r=0.83$ ). Analysis of the minimum and maximum 3D curvature values,  $k_{\text{max}}$  and  $k_{\text{min}}$ , resulted in similar correlations with the invasive data ( $r$ : 0.72 and 0.80). Mean septal 3D curvature,  $k_{\text{mean}}$ , also showed a strong linear relationship with echo Doppler derived RVSP ( $r=0.75$ ).

#### 4. Discussion and conclusions

Accurate quantification of pulmonary artery pressures is critical to the management of patients with PH [8]. Although it has long been recognized that systolic flattening and abnormal motion of the IVS, seen on both echocardiographic [9] and cine CMR images [3-5], are signs of increased pulmonary arterial pressures, this finding is not routinely used to quantify these pressures. This study constitutes the first attempt to quantify the shape and deformation of the interventricular septum using 3D analysis of CMR images obtained in patients with PH.

Because in these patients LV shape is predominantly affected locally (septal deformation), the conventional global measures of LV volume and shape may not necessarily be expected to differentiate normal from abnormal ventricles. Indeed, our measurements of LV volume and sphericity confirmed that regional analysis targeting the IVS is necessary to differentiate normal ventricles from those affected by PH, as well as those with different degrees of PH. Moreover, because our analysis is dynamic and includes all consecutive phases of the cardiac cycle, it provides information on temporal patterns of changes in septal curvature throughout the cardiac cycle, which were found to differ between normal subjects and patients with moderate and severe PH, as well as between these two subgroups of patients. Furthermore, we found that septal 3D curvature correlated well with both the invasive and non-invasive measures of the degree of PH, including both pulmonary arterial pressures, PVR and RVSP.

One limitation of our technique is that it relies on the availability of a reconstructed LV endocardial surface, which is based on subjective multi-plane and multi-phase initialization, tracing and corrections, and may thus be prone to inter-measurement variability. We used commercial software for 3D surface reconstruction and did not test its reproducibility, since this study focused on the 3D analysis of septal curvature, which is fully automated once the endocardial surface is defined.

In summary, the results of this study demonstrated that, in addition to its known ability to accurately evaluate RV volumes and function, CMR imaging could also provide quantitative information on 3D curvature of the IVS and its patterns of changes throughout the cardiac cycle, which reflects the extent of ventricular remodeling according to the severity of PH. This complementary information may further improve the utility of CMR imaging in the evaluation of patients with PH.

#### References

- [1] Arcasoy SM, Christie JD, Ferrari VA, et al: Echocardiographic assessment of pulmonary hypertension in patients with advanced lung disease. *Am J Respir Crit Care Med* 2003; 167:735-740
- [2] Milan A, Magnino C, Veglio F: Echocardiographic Indexes for the Non-Invasive Evaluation of Pulmonary Hemodynamics. *J Am Soc Echocardiogr* 2010; 23:225-239
- [3] Roeleveld RJ, Marcus JT, Faes TJ, et al: Interventricular septal configuration at MR imaging and pulmonary arterial pressure in pulmonary hypertension. *Radiology* 2005; 234:710-717
- [4] Dellegrottaglie S, Sanz J, Poon M, et al: Pulmonary hypertension: accuracy of detection with left ventricular septal-to-free wall curvature ratio measured at cardiac MR. *Radiology* 2007; 243:63-69
- [5] Alunni JP, Degano B, Arnaud C, et al: Cardiac MRI in pulmonary artery hypertension: correlations between morphological and functional parameters and invasive measurements. *Eur Radiol* 2010; 20:1149-1159
- [6] Abaci A, Kabukcu M, Ovunc K, et al: Comparison of the three different formulas for Doppler estimation of pulmonary artery systolic pressure. *Angiology* 1998; 49:463-470
- [7] Garimella RV, Swartz BK: *Curvature Estimation for Unstructured Triangulations of Surfaces*. Los Alamos, New Mexico, Los Alamos National Library, 2003.
- [8] McLaughlin VV, Archer SL, Badesch DB, et al: ACCF/AHA 2009 expert consensus document on pulmonary hypertension a report of the American College of Cardiology Foundation Task Force on Expert Consensus Documents and the American Heart Association developed in collaboration with the American College of Chest Physicians. *J Am Coll Cardiol* 2009; 53:1573-1619
- [9] Ricciardi MJ, Bossone E, Bach DS, Armstrong WF, Rubenfire M: Echocardiographic predictors of an adverse response to a nifedipine trial in primary pulmonary hypertension: diminished left ventricular size and leftward ventricular septal bowing. *Chest* 1999; 116:1218-1223

Address for correspondence:

Victor Mor-Avi, PhD  
 University of Chicago MC5084,  
 5841 S. Maryland Ave., Chicago Illinois 60637.  
 E-mail: vmoravi@medicine.bsd.uchicago.edu